Atomic Dynamics in Simple Liquid: de Gennes Narrowing Revisited

Bin Wu, Takuya Iwashita, and Takeshi Egami

Atomic Dynamics in Simple Liquid: De Gennes Narrowing Revisited

Bin Wu[1,†], Takuya Iwashita[2,#], Takeshi Egami[1,2,3,*]

[1] Department of Physics and Astronomy, Shull Wollan Center – Joint Institute of Neutron Science, University of Tennessee, Knoxville, Tennessee 37996, USA

[2] Department of Materials Science and Engineering, University of Tennessee, Knoxville, Tennessee 37996, USA

[3] Oak Ridge National Laboratory, Oak Ridge, Tennessee 37831, USA

[†] Present address: Neutron Scattering Division, Oak Ridge National Laboratory, Oak Ridge, Tennessee 37831, USA

[#] Present address: Department of Electrical and Electronic Engineering, Oita University, Oita 870-1192, Japan

* To whom correspondence should be addressed: egami@utk.edu

Abstract

The de Gennes narrowing phenomenon is frequently observed by neutron or x-ray scattering measurements of the dynamics of complex systems, such as liquids, proteins, colloids, and polymers. The characteristic slowing down of dynamics in the vicinity of the maximum of the total scattering intensity is commonly attributed to enhanced cooperativity. In this Letter, we present an alternative view on its origin through the examination of the time-dependent pair correlation function, the Van Hove correlation function, for a model liquid in two, three, and four dimensions. We find that the relaxation time increases monotonically with distance and the dependence on distance varies with dimension. We propose a heuristic explanation of this dependence based on a simple geometrical model. This finding sheds new light on the interpretation of the de Gennes narrowing phenomenon and the α-relaxation time.

The dynamics of complex soft matter, including polymers [1-4], biological matter [5-7], colloids [8, 9] and various liquids [10, 11], is frequently measured by scattering experiments, such as quasi-elastic neutron scattering (QENS), x-ray photon correlation spectroscopy (XPCS) and neutron spin echo (NSE). Often one observes that the dynamics characteristically slows down in the range of Q, the momentum transfer, where the total scattering intensity, $S(Q)$, reaches maximum. This phenomenon is widely known as the de Gennes narrowing [12], and is usually interpreted as the sign of enhanced cooperative dynamics. Despite the ubiquity of this phenomenon, details of the dynamics are rarely discussed, particularly in real space. In this Letter we suggest that the de Gennes narrowing could originate from a simple geometrical reason, and its observation does not necessarily imply the presence of collective dynamics.

In 1954, Van Hove showed that the double differential cross section measured by inelastic x-ray or neutron scattering experiments are the Fourier transform of density correlations in space and time, by generalizing the concept of pair distribution function (PDF) [13]. The time-displaced PDF, $G(r, t)$, where r is distance and t is time, is now known as the Van Hove correlation function. It can be partitioned into the self- and distinct-parts, defined as $G_s(r, t)$ and $G_d(r, t)$. The self-part tracks the positional correlation of the same particle at time t' and $t' + t$ and describes migration of a single particle. It is usually Gaussian for simple liquids [14, 15], whereas it is known to deviate considerably from the Gaussian form in deeply supercooled liquid [16-19]. On the other hand, the distinct-part records the positional correlation between different particles. At $t = 0$ $G_d(r, 0)$ is the snap-shot PDF, and as t approaches infinity the distinct-part converges asymptotically to unity. However, its relaxation process within these two temporal limits for general liquids is not understood well. Whereas for a long time the Van Hove function has been accessible only by simulation [16-20], it is now possible to determine it experimentally with high accuracy through the inelastic scattering measurements [21]. This provides additional incentive to further our understanding on the nature of the Van Hove correlation function.

3

We study model liquid iron as a representative of simple liquid using molecular dynamics simulations. The focus is placed on three dimensional (3D) simulations whereas complementary two dimensional (2D) and four dimensional (4D) simulations are also carried out to support our argument on the mechanism. We employ *NVT* ensemble, and the details regarding the simulation setup can be found in Supplementary Materials [22]. The melting point in 3D is around 2400 K and the viscosity crossover temperature denoted T_A, below which super-Arrhenius behavior occurs, is around 2000 K consistent with previous studies [27]. The distinct-part of the Van Hove correlation function is computed using eq. 1 in 3D, where $\vec{r}_i(t')$ represents the position of particle i at time t' and $\langle ..... \rangle$ means thermal averaging over the choices of t'.

$$G_d(r,t) = \frac{V}{4\pi r^2 N^2} \left\langle \sum_{i \neq j}^{N} \delta(r - |\vec{r}_i(t') - \vec{r}_j(t'+t)|) \right\rangle \tag{1}$$

A typical example obtained from 3D simulation at $T = 2500$ K is displayed in Fig 1. In panel (*a*), the result, $G_d(r, t) - 1$, is shown in a series of constant time slices. We see that at $t = 0$ the oscillations in the PDF extend to long range, and are discernible even beyond 15 Å. As time progresses the locations of peaks and valleys remain nearly the same whereas their amplitudes gradually decay to zero. However, the decay rate appears to vary with distance r. For instance, the decay of the first peak is much faster than that of the second peak although the relaxation behavior of long range peaks and valleys are unclear from this illustration because of their small amplitudes. We normalize $G_d(r, t) - 1$ through $G_d(r, 0) - 1$ and show constant r slices in panel (*b*). This plot demonstrates one of our major findings in this Letter: the relaxation time of $G_d(r, t) - 1$ has monotonic r-dependence. With larger distance, the relaxation becomes more sluggish. We find that the normalized $G_d(r, t) - 1$ can be satisfactorily described by the functional form of $\exp(-(t/\tau)^\beta)$, where τ is interpreted as the relaxation time and β quantifies contraction or stretching of the exponential. We employ this functional form to fit the normalized correlation function at selected distances and the fitting curves are shown in panel (*b*) as short dashed lines. One sees that the fitting

4

quality is quite good, except for the first peak and at the short time where a ballistic process is dominant. The first peak overshoots the zero line at $t \approx 1500$ fs and remains negative afterward within the shown temporal range although it should also converge to zero at a long-time limit. Because of this overshooting, the relaxation of the first peak cannot be described by the exponential function in contrast to the peaks and valleys at far-field. Apparently the dynamics of the atoms in the first nearest neighbor shell is too strongly correlated with the central reference particle to be described by a simple exponential function. The seemingly deteriorating fitting quality at long distance and long time is due to the statistical error in calculating the Van Hove correlation function. Nonetheless, all the r-squared parameters from fitting are better than 0.995 (see section 7 in Supplementary Materials for more details). It is important to note that the extracted relaxation time is model independent. One can alternatively determine the relaxation time by empirically monitoring the time when the normalized Van Hove function decays to $1/e$ and both methods yield identical value within statistical uncertainty.

The determined r-dependent relaxation time $\tau(r)$ at three representative temperatures is shown in Fig 2. It is clear that $\tau(r)$ increases linearly with distance, and the slope is temperature dependent. Such linear dependence was observed also for our simulations with the Lennard-Jones and Yukawa potentials, suggesting that this is a general behavior of high-temperature liquids. The value of β was also found to increase linearly with r, and is weakly dependent on temperature, as shown in Supplementary Material [22]. It is difficult to provide a full and rigorous explanation of this linearly increasing relaxation time, but we propose the following heuristic argument. By the definition of $g(r)$ in 3D, or equivalently $G_d(r, 0)$, the number of particles located within the range of r to $r + dr$ from a reference particle is on average $N(r) = 4\pi\rho_0 g(r)r^2 dr$, where ρ_0 is the number density of atoms. We note that the PDF is a spherically averaged quantity, and at large distance the PDF describes the correlation between one atom at the center and an aggregate of atoms at the distance r, rather than the direct atom-atom correlation. Based on this understanding, $\tau(r)$ then should reflect the relaxation of the aggregate of atoms and arguably scale with its fluctuations, $\Delta N(r)$. By the central limit theorem (See Supplementary Materials [22] for more details) the

5

fluctuation in the number of particles within the same radial shell is proportional to the square root of $N(r)$, hence, $\Delta N(r) \propto r\sqrt{4\pi\rho_0 g(r)}$. At far-field where $g(r) \approx 1$, $\Delta N(r)$ is consequently proportional to r, suggesting the scaling behavior of $\tau(r) \propto r$ in 3D. According to this argument the observed linearly increasing relaxation time is directly attributable to a geometrical factor, not the collectivity of dynamics. This argument can be readily tested through dimensionality dependence of the geometrical factor. In general, $\Delta N(r)$ in D-dimensional liquid should be characterized by the $(D-1)/2$ power dependence on r at far field. Thus $\tau(r)$ is expected to show $r^{0.5}$ and $r^{1.5}$ dependences in 2D and 4D respectively. To verify such prediction, the same analysis was applied also to the complementary 2D and 4D simulations at 2500 K and 3500 K respectively. We note that because the crossover temperature T_A increases with dimensionality, a higher temperature is chosen here for 4D.

We observe that $\tau(r)$ in 2D and 4D also increases with distance and indeed shows different curvatures comparing to 3D. Following the previous argument we fit the relaxation time with the power law, $\tau(r) = \tau_r \left(\dfrac{r}{r_1}\right)^{\chi} + \tau_0$, where r_1 is the position of the first peak of PDF and τ_r, τ_0, and χ are fitting parameters, at distances beyond the first peak. The fitting results are summarized in Table 1. The determined powers χ are found to be close to the expected values. We argue that the discrepancy between the fitted parameter and expected value of χ in 2D is due to the presence of robust hexatic fluctuations [28], which is not taken into consideration in the geometrical model. The uniqueness of 2D can also find support from the negligible magnitude of τ_0 in contrast to 3D and 4D. Furthermore it is conceivable that the power χ in 4D could be underestimated due to a limited r-range (see Supplementary Materials [22] for simulation setup). In order to assess the fitting quality and highlight the χ parameter, we plot $\log\{[\tau(r) - \tau_0]/\tau_r\}$ versus $\log(r/r_1)$ in Fig 3, where the slope is equal to χ. Therefore we suggest that the present results qualitatively support the previous argument: The relaxation time of the distinct Van

6

Hove correlation function is characterized by the power law dependence on distance at far-field with the power $\chi = (D\text{-}1)/2$.

Next we investigate the nature of τ_r and τ_0 from the found power law dependence of $\tau(r)$ by examining their temperature dependences in 3D, assuming $\chi = 1$. The results are shown in Fig 4. In (*a*), one sees that both τ_r and τ_0 show the Arrhenius behavior at high temperatures and become super-Arrhenius below the viscosity crossover temperature, $T_A \approx 2000K$, similar to the well-known behavior of the Maxwell relaxation time τ_M [27]. To understand the relationship among τ_r, τ_0 and τ_M, we plot their ratios as a function of temperatures in (*b*). The Maxwell relaxation time is calculated from the shear stress correlation function using the Kubo equations as in Refs [27, 29]. It is first noticed that the ratio τ_r/τ_0 is constant within the statistical uncertainty across the studied temperature range. This ratio is found be 0.55 and is dimensionality dependent; the τ_r/τ_0 ratio for 4D is around 0.18. Secondly, we see that both the τ_r/τ_M ratio and the τ_0/τ_M ratio are constant (1.55 and 2.83, respectively) at high temperatures and increase below T_A. These observations suggest that τ_r and τ_0 have the same origin, both reflecting the relaxation of density fluctuation. At high temperatures, there is only one relaxational time-scale (Maxwell relaxation time) because phonons are localized [27]. Therefore τ_r and τ_0 are proportional to τ_M. However, below T_A density fluctuation and stress fluctuation become decoupled due to the fact that phonons can propagate longer than one atomic distance [27]. As such, the proportionalities break down.

We now discuss the slowdown of dynamics at a wavevector Q corresponding to the maximum in $S(Q)$, known as the de Gennes narrowing phenomenon, from the perspective of real space dynamics. In Fig 5 (*a*), we show the relaxation time $\tau(Q)$ determined from the collective-part of the intermediate scattering function, $F_c(Q, t)$, which is the Fourier-transformation of the total Van Hove correlation function, at $T = 2500$ K in 3D. Here $\tau(Q)$ is defined as the time when $F_c(Q, t)/F_c(Q, 0)$ decays to $1/e$. It shows clear slowing down in the vicinity of the first peak of the structure factor $S(Q)$ shown in Fig 5 (*b*), as suggested by de Gennes [12]. It has long been speculated that this characteristic slowing down is due

7

to the cooperativity of dynamics at the corresponding length-scale. However, our results provide an alternative interpretation. Because $T = 2500$ K is higher than T_A, there should be no collective dynamics at this temperature. But the r-dependence of the relaxation time, $\tau(r)$, shown in Fig. 2, provides the explanation. Because $g(r)$ and $S(Q)$ are connected by the Fourier transformation, the first peak of $S(Q)$ at Q_{Max} largely generates the long-range oscillations in $g(r)$, whereas the first peak in $g(r)$ creates the high-Q part of $S(Q)$ [30]. Therefore $F_c(Q_{Max}, t)$ reflects the behaviors of the far fields of $G_d(r, t)$, which are slower. This explains why $\tau(Q_{Max})$ (= 417 fs) is much longer than the relaxation time of the first peak of the distinct-part of the Van Hove correlation function, 200 fs. On the other hand, at other wave-vectors the structure factor has both constructive and destructive interferences from the peaks and valleys of $g(r)$ (see Supplementary Materials [22] for further discussion). Consequently the relaxation of $S(Q)$ away from the first peak is dominated by the self-part of the Van Hove function. Therefore the corresponding relaxation time is much shorter than $\tau(Q_{Max})$ as shown in Fig 5. In this interpretation of the de Gennes narrowing, the reason for the characteristic slowing down is due to the linearly increasing relaxation time in the distinct-part of the Van Hove correlation function in 3D for a geometrical reason, rather than the enhanced cooperativity in collective dynamics. This analysis shows that the observation of the de Gennes slowing down does not necessarily mean the presence of collective relaxation modes. In many cases it merely reflects the geometrical factor as explained here.

This argument also raises a serious question regarding the validity of defining the α-relaxation time, τ_α, as $\tau(Q_{Max})$, as is customarily done. The reasoning is that $\tau(Q_{Max})$ represents the relaxation time of the far-field oscillations in $g(r)$, thus the structural relaxation time. However, as discussed above the longevity of the oscillations in $g(r)$ is merely the result of a geometrical factor, and the only independent parameter in simple liquids above T_A is just τ_M [27]. The popularity of $\tau(Q_{Max})$ may well originate from the fact that in the scattering experiment it is easier to determine the relaxation time at the peak of $S(Q)$. Then it is just an exemplary case of looking for a key under the lamp post. Thus in our view the so-called α-relaxation time determined as $\tau(Q_{Max})$ is not a physically meaningful parameter. In general we find it is

8

dangerous to discuss the relaxation time of the system from the intermediate scattering function, $F(Q, t)$. Our view is that only when the full Van Hove function is determined the analysis of the relaxation time in liquid becomes physically meaningful.

In conclusion, we showed that the distinct-part of the Van Hove correlation function encodes rich information regarding the dynamics of simple liquids. There are two major findings in this Letter: First, the relaxation time of the distinct Van Hove correlation function increases monotonically with distance; second, this relaxation time is found to follow a power law dependence on r with power χ close to the prediction $(D-1)/2$ at far-field. We attribute this power law dependence to a geometrical reason. Based on this reasoning, we argue that the de Gennes narrowing phenomenon does not necessarily reflect the presence of collective dynamics but could simply be due to the linearly growing $\tau(r)$ in 3D for a geometrical reason. There are still many characteristics not understood from the distinct-part of the Van Hove correlation function, such as the relaxation process of the first peak of PDF and the physical meanings of τ_r and τ_0 from the power law dependence, which will be left to the future studies using binary mixture that allows exploration on deeply supercooled regime. With the development of higher brilliance radiation sources, soon the present results can be tested through scattering experiments.

References:

1.   B. Frick and D. Richter, Science **267**, 1939 (1995).

2.   J. Colmenero, A. Arbe, G. Coddens, B. Frick, C. Mijangos, and H. Reinecke, Phys. Rev. Lett. **78**, 1928 (1997).

3.   M. Inui, S. Hosokawa, K. Matsuda, S. Tsutsui, and A. Q. R. Baron, Phys. Rev. B **77**, 224201 (2008).

4.   P. Falus, M. A. Borthwick, S. Narayanan, A. R. Sandy, and S. G. J. Mochire, Phys. Rev. Lett. **97**, 066102 (2006).

5.   Z. Wang, C. E. Bertrand, W.-S. Chiang, E. Fratini, P. Baglioni, A. Atlatas, E. Ercan Alp, and S.-H. Chen, J. Phys. Chem. B, **117**, 1186 (2013).

6.   L. Hong, N. Smolin, and J. C. Smith, Phys. Rev. Lett. **112**, 158102 (2014).

7.   M. K. Braun, M. Grimaldo, F. Roosen-Runge, I. Hoffmann, O. Czakkel, M. Sztucki, F. Zhang, F. Schreiber, T. Seydel, J. Phys. Chem. Lett. 8, 2590 (2017).

8.   L. B. Lurio, D. Lumma, A. R. Sandy, M. A. Borthwick, P. Falus, S. G. J. Mochrie, J. F. Pelletier, M. Sutton, L. Regan, A. Malik, and G. B. Stepheson, Phys. Rev. Lett. **84**, 785 (2000).

9.   K. Nygård, J. Buitenhuis, M. Kagias, K. Jefimovs, F. Zontone, and Y. Chushkin, Phys. Rev. Lett. **116**, 167801 (2016).

10.   M. Leitner, B. Sepiol, L.-M. Stadler, B. Pfau, and G. Vogl. Nat. Mater. **8**, 717 (2009).

11.   B. Ruta, G. Baldi, Y. Chushkin, B. Ruffle, L. Cristofolini, A. Fontana, M. Zanatta, and F. Nazzani, Nat. Commun. **5**, 3939 (2014).

12.   P. G. de Gennes, Physica **25**, 825 (1959).

13.   L. V. Hove, Phys. Rev. **95**, 249 (1954).

14.   A. Rahman, K. S. Singwi, and A. Sjölander, Phys. Rev. 126, 986 (1962).

15.   B. A. Dasannacharya and K. R. Rao, Phys. Rev. **137**, A417 (1965).

16.   J.-N. Roux, J. L. Barrat, and J.-P. Hansen, J. Phys.: Condens. Matter **1**, 7171 (1989).

17.   J.-L. Barrat, J.-N. Roux, and J.-P. Hansen, Chem. Phys. **149**, 197 (1990).

18.   R. Yamamoto and A. Onuki, Phys. Rev. Lett. **81,** 4915 (1998).

19. W. Kob and H. Andersen, Phy. Rev. E **51**, 4626 (1995).

20. A. Rahman, Phys. Rev. **136**, A405 (1964).

21. T. Iwashita, B. Wu, W.-R. Chen, S. Tsutsui, A. Q. R. Baron and T. Egami, *Science Advances,* **3,** e1603079 (2017).

22. See Supplemental Material [url] for (1) simulation setup, (2) variation of β with distance and temperature, (3) statistical fluctuations of $N(r)$, (4) dimensionality dependence of $\tau(r)$, (5) intermediate scattering function, (6) De Gennes narrowing, and (7) stretched exponential analysis, which includes Refs [23-26].

23. D. Srolovitz, K. Maeda, V. Vitek, and T. Egami, *Phil. Mag. A* **44**, 847 (1981).

24. S. Plimpton, *J. Comp. Phys.* **117**, 1 (1995).

25. E. B. Tadmor and R. E. Miller, *Modeling Materials: Continuum, Atomistic and Multiscale Techniques* (Cambridge University Press, Cambridge, 2012) 1st ed.

26. M. P. Allen and D. J. Tildesley, *Computer Simulation of Liquids* (Oxford University Press, New York, 1987).

27. T. Iwashita, D. M. Nicholson, and T. Egami, Phys. Rev. Lett. **110**, 205504 (2013).

28. J. M. Kosterlitz and D. J. Thouless, J. Phys. C **6,** 1181 (1973).

29. J.-P. Hansen and I. R. McDonald, *Theory of Simple Liquids* (Academic Press, Amsterdam, 2006) 3rd ed.

30. G. S. Cargill, III, Solid St. Phys. **30,** 227 (1975).

Table 1 Parameters determined from power law fitting to $\tau(r)$. The errors reflect 95% confidence bounds.

	χ	τ_r (fs)	τ_0 (fs)
2D	0.66 ± 0.14	179.10 ± 80.60	8.84 ± 111.56
3D	1.04 ± 0.16	122.30 ± 51.70	252.80 ± 94.90
4D	1.45 ± 0.20	31.18 ± 11.95	171.20 ± 23.20
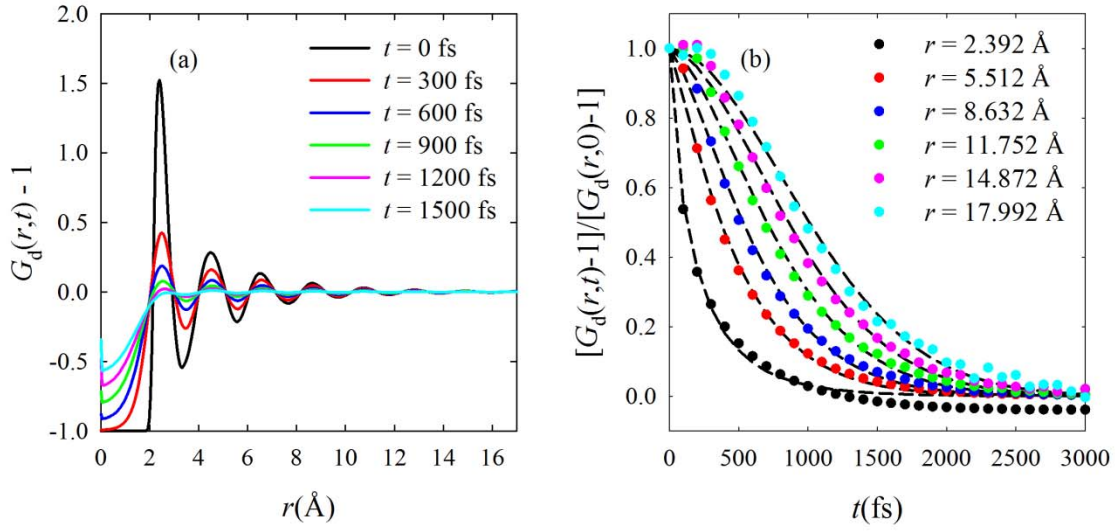
Figure 1. The distinct-part of the Van Hove correlation function, $G_d(r, t)-1$, for 3D model liquid iron at 2500 K: (a) constant t plot and (b) constant r plot. In (b), the results are normalized using respective $t = 0$ values and the normalized correlation functions are fit with $\exp(-(t/\tau)^\beta)$ shown as short dashed lines.
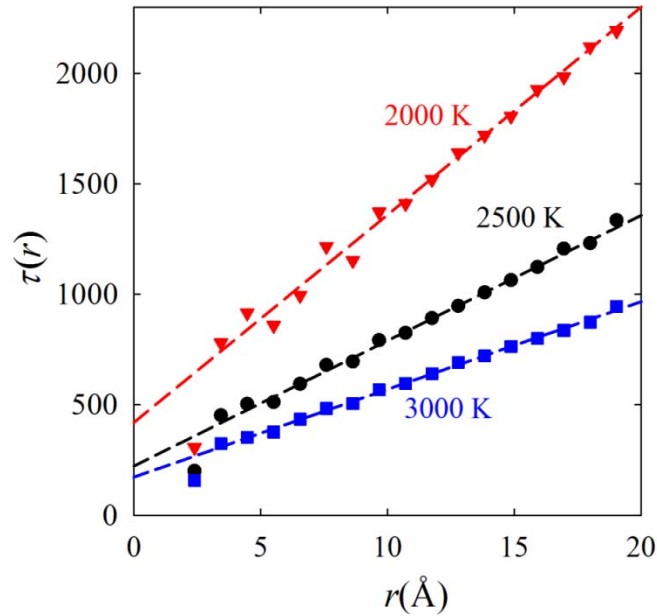

Figure 2. The relaxation time determined from $G_d(r,t)$ in 3D liquid iron at a series of distances at temperatures of 2000 K, 2500 K and 3000 K. The short-dashed straight lines serve as guides to the eyes.
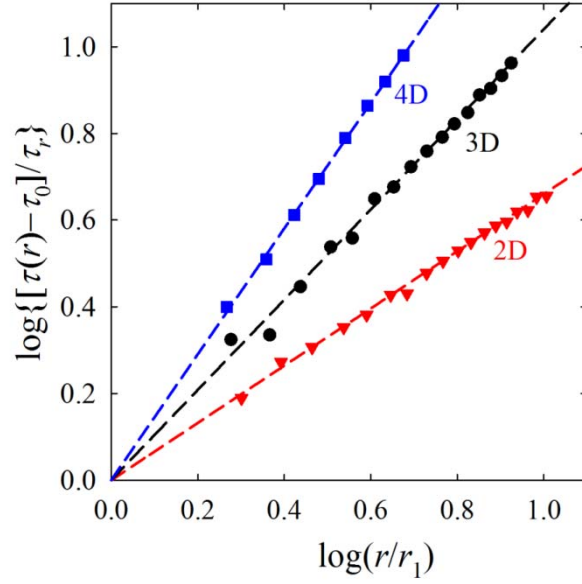
Figure 3. The *r*-dependent relaxation time $\tau(r)$ determined from the normalized distinct-part of van Hove correlation function of model liquid iron in 2D at 2500K (red triangle), 3D at 2500K (black circle), and 4D at 3500K (blue square) beyond the first peak position. The data points are shown in the form of $\log\{[\tau(r)-\tau_0]/\tau_r\}$ versus $\log(r/r_1)$ to highlight χ from the expected power law dependence, where τ_0 and τ_r are taken from Table 1. The short dashed lines serve as guides to the eye.
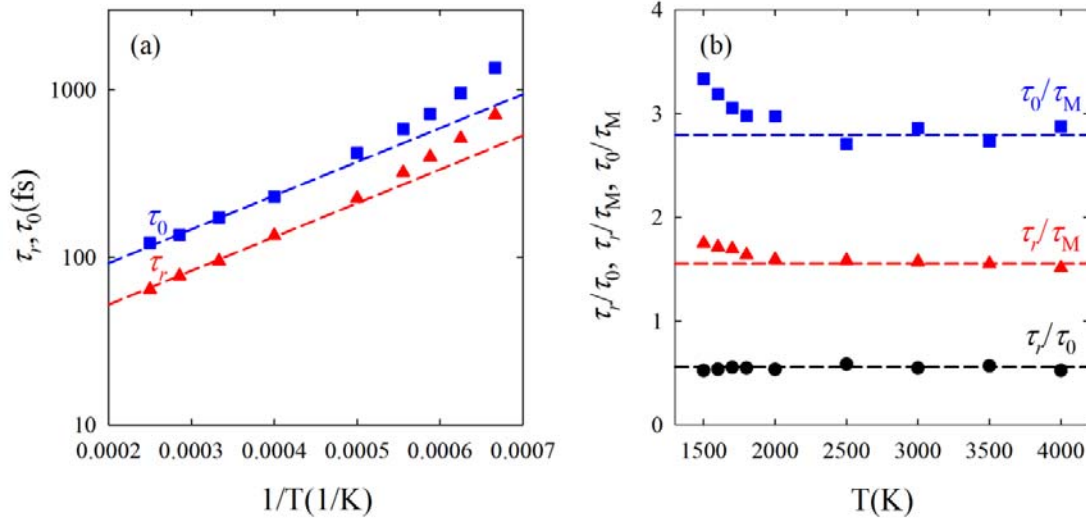

Figure 4. Temperature dependence of τ_r and τ_0 from linear fitting to the *r*-dependent relaxation time of normalized distinct-part of the Van Hove correlation function of model liquid iron in 3D. The results are shown in Arrhenius plot in (a) and ratios in (b). τ_M is Maxwell relaxation time. Short dashed lines serve as guides to the eyes.
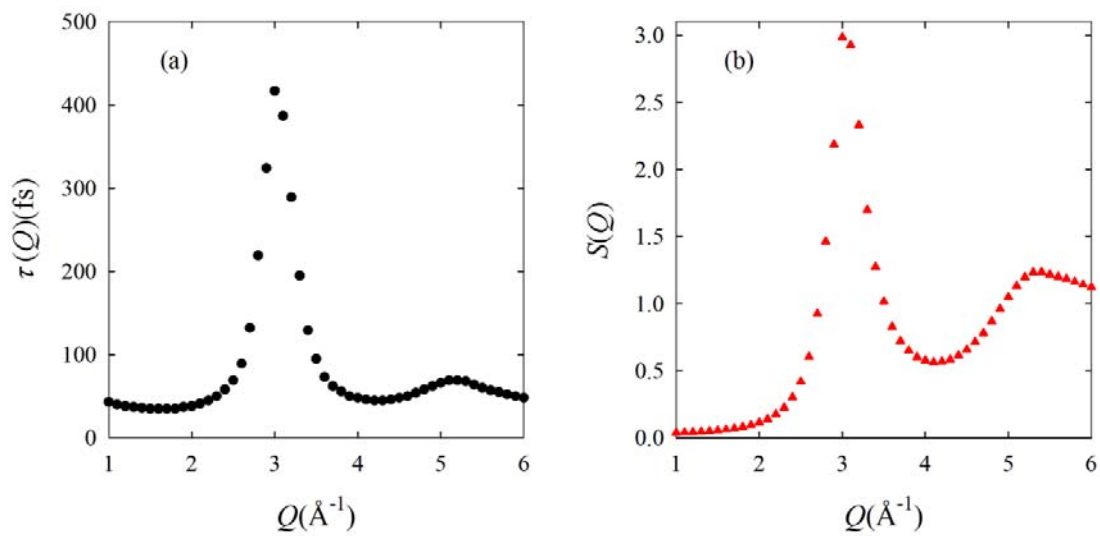
14

Figure 5 Illustration of de Gennes narrowing phenomenon: The wave-vector dependent relaxation time $\tau(Q)$ determined from the collective-part of intermediate scattering function at 2500 K in 3D liquid iron shown in (a) clearly demonstrates a characteristic slowing down in the vicinity of the peak position of $S(Q)$ shown in (b).

15